Classification of Polarimetric SAR Images Using Evolutionary RBF Neural Networks

Turker Ince*, Serkan Kiranyaz** and Moncef Gabbouj**
* turker.ince@ieu.edu.tr, *Izmir University of Economics, Izmir, Turkey*
** {serkan.kiranyaz, moncef.gabbouj}@tut.fi, *Tampere University of Technology, Tampere, Finland*

Abstract

This paper proposes an evolutionary RBF network classifier for polarimetric synthetic aperture radar (SAR) images. The proposed feature extraction process utilizes the full covariance matrix, the gray level co-occurrence matrix (GLCM) based texture features, and the backscattering power (Span) combined with the H/α/A decomposition, which are projected onto a lower dimensional feature space using principal component analysis. An experimental study is performed using the fully polarimetric San Francisco Bay data set acquired by the NASA/Jet Propulsion Laboratory Airborne SAR (AIRSAR) at L-band to evaluate the performance of the proposed classifier. Classification results (in terms of confusion matrix, overall accuracy and classification map) compared to the Wishart and a recent NN-based classifiers demonstrate the effectiveness of the proposed algorithm.

1. Introduction

Image and data classification techniques play an important role in the automatic analysis and interpretation of remote sensing data. Particularly polarimetric synthetic aperture radar (SAR) data poses a challenging problem in this field due to complexity of measured information from its multiple polarimetric channels. Recently, the number of applications which use data provided by the SAR systems having fully polarimetric capability have been increasing. Over the past decade, there has been extensive research in the area of the segmentation and classification of polarimetric SAR data. In the literature, the classification algorithms for polarimetric SAR can be divided into three main classes: 1) classification based on physical scattering mechanisms inherent in data [1], [2] 2) classification based on statistical characteristics of data [3], [4] and 3) classification based on image processing techniques [5], [6]. Additionally, there has been several works using some combinations of the above classification approaches [3], [1]. While these approaches to the polarimetric SAR classification problem can be based on either supervised or unsupervised methods, their performance and suitability usually depend on applications and the availability of ground truth.

As one of the earlier algorithms, Kong et al. [7] derived a distance measure based on the complex Gaussian distribution and used it for maximum-likelihood (ML) classification of single-look complex polarimetric SAR data. For multilook data represented in covariance or coherency matrices, Lee *et al.* [3] proposed a new unsupervised classification method based on combination of polarimetric target decomposition (specifically the Cloude and Pottier decomposition [8]) and the maximum likelihood classifier using the complex Wishart distribution. The unsupervised Wishart classifier has an iterative procedure based on the well-known *K-means* algorithm, and has become a preferred benchmark algorithm due to its computational efficiency and generally good performance. However, this classifier still has some significant drawbacks since it entirely relies on *K-means* for actual clustering, such as it may converge to local optima, the number of clusters should be fixed *a priori*, its performance is sensitive to the initialization and its convergence depends on several parameters. Recently, a two-stage unsupervised clustering based on the EM algorithm [9] is presented for classification of polarimetric SAR images. The EM algorithm estimates parameters of the probability distribution functions which represent the elements of a 9-dimensional feature vector, consisting of six magnitudes and three angles of a coherency matrix. In [10], a new wavelet-based texture image segmentation algorithm is successfully applied to unsupervised SAR image segmentation problem. More recently, neural network based approaches [11], [12] for classification of polarimetric synthetic aperture radar data have been shown to outperform other aforementioned well-known techniques. Compared with other approaches, neural network classifiers have the advantage of adaptability to the data without making *a priori* assumption of a particular probability model or distribution. However, their performance depends on the network structure, training data, initialization and parameters. In this paper, we propose evolutionary radial basis function (RBF) networks based on dynamic clustering using multi-dimensional particle swarm optimization (MD PSO) [13] for polarimetric SAR image classification. By using both polarimetric covariance matrix and polarimetric decomposition based pixel values and textural information (contrast, correlation, energy, and homogeneity) in the feature set, the classification accuracy is improved. The fully polarimetric test image of San Francisco Bay acquired by the NASA/Jet Propulsion Laboratory Airborne SAR (AIRSAR) was

chosen to demonstrate performance of the proposed MD-PSO based evolutionary RBF classifier and its classification results are compared to the Wishart classifier.

2. Polarimetric SAR Data Processing

Polarimetric radars measure the complex scattering matrix *S* produced by a target under study with the objective to infer its physical properties. Assuming linear horizontal and vertical polarizations for transmitting and receiving, *S* can be expressed as

$$S = \begin{bmatrix} S_{hh} & S_{hv} \\ S_{vh} & S_{vv} \end{bmatrix} \quad (1)$$

Reciprocity theorem applies in a monostatic system configuration, $S_{hv} = S_{vh}$. For coherent scatterers only, the decompositions of the measured scattering matrix *S* can be employed to characterize the scattering mechanisms of such targets. Alternatively, the second order polarimetric descriptors of the 3x3 average polarimetric covariance $\langle [C_3] \rangle$ and the coherency $\langle [T_3] \rangle$ matrices can be employed to extract physical information from the observed scattering process. The elements of the covariance matrix can be written in terms of three unique polarimetric components of complex scattering matrix:

$$\begin{aligned} C_{11} &= S_{hh} S_{hh}^*, \quad C_{21} = S_{hh}^* S_{hv} \\ C_{22} &= S_{hv} S_{hv}^*, \quad C_{32} = S_{hv}^* S_{vv} \\ C_{33} &= S_{vv} S_{vv}^*, \quad C_{31} = S_{hh}^* S_{vv} \end{aligned} \quad (2)$$

For single-look processed polarimetric SAR data, the three polarimetric components (HH, HV, and VV) has a multivariate complex Gaussian distribution and the complex covariance matrix form has a complex Wishart distribution [14]. Due to presence of speckle noise and random vector scattering from surface or volume, polarimetric SAR data are often multi-look processed by averaging *n* neighboring pixels.

Cloude-Pottier decomposition [8] is based on eigenanalysis of the polarimetric coherency matrix, $\langle [T] \rangle$:

$$\langle T \rangle = \lambda_1 e_1 e_1^{*T} + \lambda_2 e_2 e_2^{*T} + \lambda_3 e_3 e_3^{*T} \quad (3)$$

where $\lambda_1 > \lambda_2 > \lambda_3 \geq 0$ are real eigenvalues and the corresponding orthonormal eigenvectors e_i (representing three scattering mechanisms) are

$$e_i = e^{i\phi_i} \left[\cos \alpha_i, \sin \alpha_i \cos \beta_i e^{i\delta_i}, \sin \alpha_i \sin \beta_i e^{i\gamma_i} \right]^T \quad (4)$$

Cloude and Pottier defined entropy *H* and average of alpha angle, $\bar{\alpha}$ for analysis of the physical information related to the scattering characteristics of a medium:

$$H = -\sum_{i=1}^{3} p_i \log_3 p_i \qquad \text{where} \qquad p_i = \frac{\lambda_i}{\sum_{i=1}^{3} \lambda_i} \quad (5)$$

$$\bar{\alpha} = \sum_{i=1}^{3} p_i \alpha_i \quad (6)$$

For a multi-look coherency matrix, the entropy, $0 \leq H \leq 1$, represents the randomness of a scattering medium between isotropic scattering (*H* =0) and fully random scattering (*H* =1), while the average alpha angle can be related to target average scattering mechanisms from single-bounce (or surface) scattering $(\bar{\alpha} \approx 0)$ to dipole (or volume) scattering $(\bar{\alpha} \approx \pi/4)$ to double-bounce scattering $(\bar{\alpha} \approx \pi/2)$. Due to basis invariance of the target decomposition, *H* and α are roll invariant hence they do not depend on orientation of target about the radar line of sight. Additionally, information about target's total backscattered power can be determined by the *span* as

$$span = \sum_{i=1}^{3} \lambda_i \quad (7)$$

H, $\bar{\alpha}$, and *span* calculated by the above noncoherent target decomposition method have been widely used as the main polarimetric features of a scatterer in many target classification schemes.

3. Feature Extraction

The proposed feature extraction process utilizes the complete covariance matrix information, the gray level co-occurrence matrix (GLCM) based texture features, and the backscattering power (*span*) combined with the $H/\alpha/A$ decomposition [8]. As suggested by the previous studies [15], [11] appropriate texture measures for SAR imagery based on the gray level co-occurrence probabilities are included in the feature set to improve its discrimination power and classification accuracy. In this study, *contrast*, *correlation*, *energy*, and *homogeneity* features are extracted from normalized GLCMs which are calculated using interpixel distance of 2 and averaging over four possible orientation settings ($\theta = 0^o, 45^o, 90^o, 135^o$).

To reduce the dimensionality (and redundancy) of input feature space, the principal components transform is applied and the most principal components (in this paper, ten principal components are selected) are then selected as features.

4. Evolutionary RBF Networks

An artificial neural network (ANN) consists of a set of connected processing units, usually called neurons or nodes. ANNs can be described as directed graphs, where each node performs some activation function to its inputs and then gives the result forward to be the input of some other neurons until the output neurons are reached. ANNs can be divided into feedforward and recurrent networks according to their connectivity. In a recurrent ANN there can be backward loops in the network structure, while in feedforward ANNs such loops are not allowed. A popular type of feedforward ANN is the RBF network [16], which has always two layers in addition to the passive input layer: a hidden layer of RBF units and a linear output layer. Only the output layer has connection weights and biases. The activation function of the k^{th} RBF unit is defined as,

$$y_k = \varphi\left(\frac{\|X - \mu_k\|}{\sigma_k^2}\right), \qquad (8)$$

where φ is a radial basis function or, in other words, a strictly positive radially symmetric function, which has a unique maximum at N-dimensional center μ_k and whose value drops rapidly close to zero away from the center. σ_k is the width of the peak around the center μ_k. The most commonly used activation function in RBF networks is the Gaussian basis function.

In an earlier work [17], multi-dimensional particle swarm optimization (MD PSO) has been successfully used to evolve multi-layer perceptrons (MLPs), that is, the automatic design of the feed-forward ANNs and the search is carried out over all possible network configurations within the specified architecture space. In [17], no assumption was made about the number of (hidden) layers and none of the network properties (e.g. feed-forward or not, differentiable activation function or not, etc.) is an inherent constraint of this scheme. In the current work, our approach for evolutionary RBF networks is that the dynamic clustering using MD PSO with FGBF determines of the optimal number of Gaussian neurons with their correct parameters (centroids and variances). Afterwards, backpropagation (BP) can conveniently be used to compute the remaining network parameters, weights (w) and bias (θ) of the each output layer neuron. Further details for MD PSO and FGBF and their mutual application for evolutionary design of ANNs (or specifically the RBF networks) can be obtained from [17].

5. Experimental Results

The NASA/Jet Propulsion Laboratory Airborne SAR (AIRSAR) L-band data of the San Francisco Bay is used for performance evaluation of the proposed evolutionary RBF classifier. The original four-look fully polarimetric SAR data of the San Francisco Bay, having a dimension of 900x1024 pixels, provides good coverage of both natural (sea, mountains, forests, etc.) and man-made targets (buildings, streets, parks, golf course, etc.) with a more complex inner structure. In this study, the sub-area with size 600x600 is extracted and used for the purpose of comparing the classification results with the Wishart [3] and the NN-based [11] classifiers. The aerial photographs for this area which can be used as ground-truth are provided by the TerraServer Web site [18]. In this study, the speckle filter suggested by Lee *et al.* [19] is employed with 5x5 window to preserve the texture information as recommended.

The same training and testing areas for three classes, the sea (15810, 6723 pixels respectively), urban areas (9362, 6800), and the vegetated zones (5064, 6534) which are manually selected in an earlier study [11] are also used for training and testing of the proposed evolutionary classifier in this study. The confusion matrix of the proposed method on the training and testing areas are given in Table 1. The classification accuracy values are averaged over 10 independent runs. From the results, the main drawback of the proposed method is the separation of vegetated zones from urban areas. Compared to two other competing techniques, the proposed method is able to differentiate better the uniform areas corresponding to main classes of scattering such as the ocean, vegetation, and building areas.

In Table 2, the overall accuracies for the three competing methods, the Wishart Maximum Likelihood (WML) classifier [3], the NN-based classifier [11], and the proposed evolutionary RBF classifier, in training and testing areas are compared. The proposed method is superior to the WML method with higher accuracies in both training and testing areas, and has the highest overall testing accuracy (98.9%) in all three techniques.

The classification map of the whole image produced by the proposed classifier is shown in Fig. 1.

TABLE I
Summary table of pixel-by-pixel classification results of the proposed method for the training and testing datasets

	Training data			**Test data**		
	Sea	**Urb**	**Veg**	**Sea**	**Urb**	**Veg**
Sea	**14265**	**3**	**0**	**6803**	**1**	**0**
Urb	**8**	**9409**	**38**	**5**	**6924**	**31**
Veg	**2**	**122**	**4469**	**6**	**192**	**6771**

TABLE II
Overall performance comparison (in percent)

Method	Training Area	Testing Area
WML [3]	97.23	96.16
NN [11]	**99.42**	98.64
Proposed Method	99.40	**98.9**

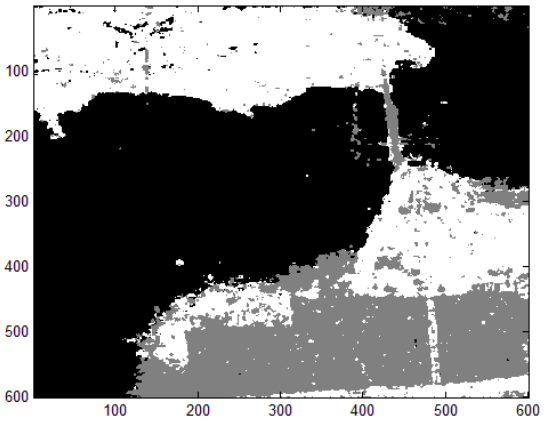

Figure 1: The classification results of the proposed technique on the whole image (black denotes sea, gray urban areas, white vegetated zones).

5. Conclusions

In this paper, the evolutionary RBF network classifier for the classification of polarimetric SAR data has been proposed. The promising results were obtained for the San Francisco dataset and compared to the Wishart and NN-based (3-layer MLP) classifiers.

References

[1] E. Pottier and J.S. Lee, "Unsupervised classification scheme of POLSAR images based on the complex Wishart distribution and the H/A/alpha-Polarimetric decomposition theorem," in Proc. of the 3rd EUSAR 2000 Conf., May 2000.

[2] J. J. van Zyl, "Unsupervised classification of scattering mechanisms using radar polarimetry data*," IEEE Trans. Geosci. Remote Sensing*, vol. 27, pp. 36–45, Jan. 1989.

[3] J. S. Lee, M. R. Grunes, T. Ainsworth, L.-J. Du, D. Schuler, and S. R. Cloude, "Unsupervised classification using polarimetric decomposition and the complex Wishart classifier," *IEEE Trans. Geosci. Remote Sens.*, vol. 37, no. 5, pp. 2249–2257, Sep. 1999.

[4] Y. Wu, K. Ji, W. Yu, Y. Su, "Region-based classification of polarimetric SAR images using Wishart MRF," *IEEE Geosci. Rem. Sens. Lett.*, vol. 5, no. 4, pp. 668-672, 2008.

[5] C. P. Tan, K. S. Lim, H. T. Ewe, "Image processing in polarimetric SAR images using a hybrid entropy decomposition and maximum likelihood (EDML) ," In Proc. Int. Symposium on Image and Signal Processing and Analysis (ISPA), pp. 418–422, Sep. 2007.

[6] Zhen Ye, Cheng-Chang Lu, "Wavelet-Based Unsupervised SAR Image Segmentation Using Hidden Markov Tree Models," In Proc. of the16th International Conference on Pattern Recognition (ICPR'02), vol. 2, pp. 20729, 2002.

[7] J. A. Kong, A. A. Swartz, H. A. Yueh, L. M. Novak, and R. T. Shin, "Identification of terrain cover using the optimum polarimetric classifier," *J. Electromagn. Waves Applicat.*, vol. 2, no. 2, pp. 171–194, 1988.

[8] S. R. Cloude and E. Pottier, "An entropy based classification scheme for land applications of polarimetric SAR," *IEEE Trans. Geosci. Remote Sensing*, vol. 35, pp. 68–78, Jan. 1997.

[9] K. U. Khan, J. Yang, and W. Zhang, "Unsupervised classification of polarimetric SAR images by EM algorithm," *IEICE Transactions on Communications*, vol. 90, no.12, pp. 3632-3642, 2007.

[10] Zhen Ye, Cheng-Chang Lu, "Wavelet-Based Unsupervised SAR Image Segmentation Using Hidden Markov Tree Models," In Proc. of the16th International Conference on Pattern Recognition (ICPR'02), vol. 2, pp. 20729, 2002.

[11] Y. D. Zhang, L.-N. Wu, and G. Wei, "A new classifier for polarimetric SAR images," *Progress In Electromagnetics Research*, PIER 94, pp. 83-104, 2009.

[12] S. Y. Yang, M. Wang, and L. C. Jiao, "Radar target recognition using contourlet packet transform and neural network approach," *Signal Processing*, vol. 89, no. 4, pp. 394-409, 2009.

[13] S. Kiranyaz, T. Ince, A. Yildirim and M. Gabbouj, "Fractional Particle Swarm Optimization in Multi-Dimensional Search Space," *IEEE Transactions on Systems, Man, and Cybernetics – Part B*, in Press, doi: 10.1109/TSMCB.2009.2015054, 2009.

[14] J.S. Lee, M.R. Grunes, and R. Kwok, "Classification of multi-look polarimetric SAR imagery based on complex Wishart distribution," *Int. J. Rem. Sens.*, vol. 15, no. 11, pp. 2299-2311, 1994.

[15] D. A. Clausi, "An Analysis of Co-occurrance Texture Statistics as a Function of Grey Level Quantization," Canadian J. Remote Sensing, vol.28, no. 1, pp. 45-62, 2002.

[16] T. Poggio and F. Girosi, "A theory of networks for approximation and learning," A.I. Memo No. 1140, M.I.T. A.I Lab, 1989.

[17] S. Kiranyaz, T. Ince, A. Yildirim and M. Gabbouj, "Evolutionary Artificial Neural Networks by Multi-Dimensional Particle Swarm Optimization," Neural Networks, vol. 22, no. 10, pp. 1448-1462, 2009.

[18] U.S. Geological Survey Images. [Online]. Available: http://terraserver-usa.com

[19] J. S. Lee, M. R. Grunes and G. de Grandi, "Polarimetric SAR speckle filtering and its implications for classification," *IEEE Trans. Geosci. Remote Sensing*, vol. 37, no. 5, pp. 2363–2373, 1999.